Atmospheric Research 197 (2017) 370–378

Contents lists available at ScienceDirect

Atmospheric Research

journal homepage: www.elsevier.com/locate/atmosres

Aerosol optical properties at rural background area in Western Saudi Arabia

H. Lihavainen[a,*], M.A. Alghamdi[b], A. Hyvärinen[a], T. Hussein[c], K. Neitola[a], M. Khoder[b], A.S. Abdelmaksoud[b], H. Al-Jeelani[b], I.I. Shabbaj[b], F.M. Almehmadi[b]

[a] Finnish Meteorological Institute, Finland
[b] Department of Environmental Sciences, Faculty of Meteorology, Environment and Arid Land Agriculture, King Abdulaziz University, P. O. Box 80208, Jeddah 21589, Saudi Arabia
[c] University of Helsinki, Department of Physics, Finland

ABSTRACT

To derive the comprehensive aerosol in situ characteristics at a rural background area in Saudi Arabia, an aerosol measurements station was established to Hada Al Sham, 60 km east from the Red Sea and the city of Jeddah. The present sturdy describes the observational data from February 2013 to February 2015 of scattering and absorption coefficients, Ångström exponents and single scattering albedo over the measurement period. The average scattering and absorption coefficients at wavelength 525 nm were 109 ± 71 Mm^{-1} (mean ± SD, at STP conditions) and 15 ± 17 Mm^{-1} (at STP conditions), respectively. As expected, the scattering coefficient was dominated by large desert dust particles with low Ångström scattering exponent, 0.49 ± 0.62. Especially from February to June the Ångström scattering exponent was clearly lower (0.23) and scattering coefficients higher (124 Mm^{-1}) than total averages because of the dust outbreak season. Aerosol optical properties had clear diurnal cycle. The lowest scattering and absorption coefficients and aerosol optical depths were observed around noon. The observed diurnal variation is caused by wind direction and speed, during night time very calm easterly winds are dominating whereas during daytime the stronger westerly winds are dominating (sea breeze). Positive Matrix Factorization mathematical tool was applied to the scattering and absorption coefficients and $PM_{2.5}$ and coarse mode (PM_{10}–$PM_{2.5}$) mass concentrations to identify source characteristics. Three different factors with clearly different properties were found; anthropogenic, BC source and desert dust. Mass absorption efficiencies for BC source and desert dust factors were, 6.0 $m^2 g^{-1}$ and 0.4 $m^2 g^{-1}$, respectively, and mass scattering efficiencies for anthropogenic (sulphate) and desert dust, 2.5 $m^2 g^{-1}$ and 0.8 $m^2 g^{-1}$, respectively.

1. Introduction

Atmospheric aerosol particles are recognized as one of the most variable components in the Earth's atmosphere. They affect the Earth's radiative balance and climate directly by scattering and absorbing solar radiation (Charlson et al., 1992; Haywood and Shine, 1995), and indirectly changing the microphysical properties of clouds (Kaufman et al., 2005). The uncertainties in various climate effects of aerosols continue to be the largest uncertainty in the total, global radiative forcing estimate (IPCC, 2013). Aerosols are also known to cause adverse health effects (e.g. Schwarze et al., 2006).

Aerosol optical properties and non-aerosol properties which influence (e.g. surface albedo and solar declination angle) are key factors when investigating the direct radiative effects of atmospheric aerosols. Because of their various sources and short life-time, the properties of these aerosols may vary significantly both temporally and spatially. In addition to the changes occurring on short time-scales, the aerosol optical properties also vary on decadal scales, especially at lower latitudes (Collaud Coen et al., 2013). To reduce the uncertainties associated with the atmospheric aerosol effects in climate systems, detailed observations on the temporal and spatial variability of different aerosol properties and sources is required.

The Arabian Peninsula is one of the strongest aerosol particle source areas, both natural and anthropogenic, in the world. As a part of the so called dust belts, natural aerosols are dominated by desert dust which can be transported over large distances (Prospero et al., 2002). Dust outbreaks and storms affect strongly both aerosol physical and optical properties causing large perturbation into the radiation energy balance and air quality (e.g. Alam et al., 2014). Furthermore, there are considerable anthropogenic emissions mainly from road traffic, petroleum industry and local constructions (Khodeir et al., 2012). The size distributions, optical properties, and physico-chemical properties of

* Corresponding author.
E-mail address: heikki.lihavainen@fmi.fi (H. Lihavainen).

http://dx.doi.org/10.1016/j.atmosres.2017.07.019
Received 8 November 2016; Received in revised form 6 June 2017; Accepted 18 July 2017
Available online 19 July 2017

aerosol particles are highly variable in such regions.

While a number of studies have investigated the properties of aerosol particles over the Arabian Sea and Indian Ocean (Johansen et al., 1999; Lelieveld et al., 2001; Ramanathan et al., 2007) the properties of aerosol particles in the Arabian Peninsula region has remained mostly unstudied until very recently. However, the most of the studies of optical properties are based on either ground (e.g. Kim et al., 2011; Osipov et al., 2015) or satellite based (e.g. Sabbah et al., 2012) remote sensing.

In order to get more insight in aerosol characteristics and behavior, the Finnish Meteorological Institute, together with the King Abdulaziz University and the University of Helsinki, established a rural background measurement station to conduct a unique, long term observational study in the western Saudi Arabia. To our knowledge this is the first long term study of in situ measured aerosol optical properties at rural background area at Arabian Peninsula. Firstly, our aim is to present seasonal and diurnal variation of aerosol optical properties and their relationships with other measured parameters at the site. Secondly, we applied positive matrix factorization (PMF) to identify different source characteristic for aerosol optical properties.

2. Materials and methods

2.1. Measurements

Detailed descriptions of the station and the measurement program are given in Lihavainen et al. (2016), and only a short description is given here. The measurement station was located at rural background site at Hada Al Sham (21.802° North, 39.729° East, 254 m a.s.l.), Fig. 1. The site is situated about 60 km east of the coast of the Red Sea and the city of Jeddah with a population of around 3.4 million and 43 km north of city of Mecca with a population of around 1.3 million. The station was located in King Abdulaziz University's Agriculture Research Station. Measurements of the aerosol properties were conducted from November 2012 to February 2015. In situ data reported here is from February 2013 to February 2015 due to a malfunction in the measurement setup preventing proper observations. The measurement period of AOD was from October 2012 to June 2014. There are few longer data gaps due to malfunction of the instruments.

Aerosol scattering coefficient at three wavelengths (450, 525 and 635 nm) were measured with Ecotech Aurora Nephelometer. The nephelometer was full calibrated with CO_2 and filtered air about once in two months and zero adjusted with filtered air (zero adjust) every 3 h. There was an unsuccessful calibration of the nephelometer that caused incorrect measurement values from June to August 2013. The data from this time period was successfully corrected using raw measurement values and calibration coefficients from earlier calibrations. Aerosol absorption coefficient at seven wavelengths (370, 470, 520, 590, 660, 880, and 950 nm) was measured with Mageé Scientific AE31 Aethalometer. The inlet to these instruments had PM_{10} cut-off nozzle. The sample air was dried with twin diffusion dryer prior entering to the instruments.

Other measurements at the station included PM_{10}, $PM_{2.5}$, aerosol size distribution from 7 nm to 10 μm, weather parameters (temperature, relative humidity pressure, wind speed and direction) and Aerosol Optical Depth (AOD) with Cimel CE-318 sun photometer as part of AERONET measurement program (Holben et al., 1998).

2.2. Data processing

The data was first quality checked against peculiar events, like instrument malfunction, which were removed from data set. The time resolution of the optical properties measurements was 5 min. Black carbon concentration and absorption coefficients were measured with Aethalometer at seven wavelengths. The Aethalometer absorption measurement is known to suffer from filter loading artifacts. These artifacts can be corrected using different methods. Here, the approach presented by Weingartner et al. (2003) together with the recent GAW recommendation (WMO/GAW report no. 227, 2016) was used. Non idealities due to non-lambertian and truncation errors in the Nephelometer were corrected using the method described by Müller et al. (2011).

Aerosol in situ data reported here are converted to standard temperature and pressure (STP) conditions (0 °C and 1013 hPa). Also all the figures are in STP conditions. Hourly averages of measurement parameters were calculated if > 50% of the data existed inside the hour in question. Monthly averages were calculated if > 30% of data was available. Diurnal variations as well as variation with meteorological parameters of aerosol optical properties were calculated as an average over the whole measurement period if > 100 data points existed in the

Fig. 1. Location of the measurement site. Map and satellite image are from maps.google.fi.

Table 1
Mean, standard deviation, 10-, 50- and 90 percentiles, and data coverage of various measured parameter over the measurement period. σ_{sca} and σ_{abs} are in Mm^{-1}.

	Mean ± std.	Percentiles			Data coverage (%)
		10	50	90	
σ_{sca} (450 nm)	116 ± 72	49	103	195	89
σ_{sca} (525 nm)	109 ± 71	45	96	181	89
σ_{sca} (635 nm)	102 ± 113	40	86	172	89
σ_{abs} (450 nm)	18 ± 19	5	11	40	87
σ_{abs} (525 nm)	15 ± 17	4	9	35	87
σ_{abs} (635 nm)	13 ± 15	3	8	30	87
SSA (450 nm)	0.87 ± 0.09	0.73	0.90	0.94	79
SSA (525 nm)	0.88 ± 0.09	0.74	0.91	0.95	79
SSA (635 nm)	0.88 ± 0.09	0.75	0.91	0.96	79
$\mathring{a}_{sca}$	0.49 ± 0.62	− 0.36	0.54	1.26	89
$\mathring{a}_{abs}$	0.97 ± 0.29	0.71	0.93	1.3	87
AOD_{500}	0.35 ± 0.20	0.12	0.31	0.62	
$\mathring{a}_{ext}$ (440–675 nm)	0.72 ± 0.46	0.20	0.65	1.29	
σ_{sca} (550 nm)	107 ± 72	44	93	178	89

hour or the weather parameter bin in question. If the sample air in the instruments had relative humidity above 50% the data was excluded from further analysis (WMO/GAW report no. 227, 2016).

The aethalometer and nephelometer measure the aerosol optical properties at slightly different wavelengths. For further analysis, the absorption coefficients were calculated to the same wavelengths as the nephelometer is measuring (450, 525 and 635 nm) by fitting a curve

$$\log \sigma_{abs} = -\mathring{a}_{abs} \log \lambda + C \quad (1)$$

to the absorption coefficient at different wavelengths (370–950 nm). In Eq. (1) λ refers to the wavelength, σ_{abs} to absorption coefficient, *C* is a constant irrelevant to this work and $\mathring{a}_{abs}$ is a constant called the absorption Ångström exponent and it describes the wavelength dependency of absorption. It is sometimes used to characterize some of the absorbing species (Kirchstetter et al., 2004; Bergstrom et al., 2007). For example, vehicle exhaust typically yields $\mathring{a}_{abs} \approx 1$, whereas for the biomass smoke or desert dust the value may reach values in excess of 2. Mixed aerosols of BC, biomass and desert dust smoke would give somewhere in the range 1–3. $\mathring{a}_{abs}$ values < 1 are routinely observed in ambient measurements (Bergstrom et al., 2007; Lack et al., 2008), this is theoretically predicted for BC spheres that are larger than ~ 150 nm (Lack and Cappa, 2010).

The scattering Ångström exponent describing the wavelength dependency of scattering over the measured wavelength range (450–635 nm), $\mathring{a}_{sca}$, was calculated by fitting a curve $\log \sigma_{sca} = -\mathring{a}_{sca} \log \lambda + C$ to the data. *C* is again a fitting constant irrelevant to this work. A large value of $\mathring{a}_{sca}$ refers to a particle size distribution with scattering dominated by submicron particles, whereas a size distribution dominated by coarse particles has typically a small value of $\mathring{a}_{sca}$. For aerosol particles with a volume mean diameter of 1.5 μm or larger (coarse), $\mathring{a}_{sca}$ is zero or negative, and for particles of < 1 μm diameter (fine), it is 1 or greater (Seinfeld and Pandis, 1998).

Aerosol single scattering coefficient (*SSA*) was calculated with following equation

$$SSA = \frac{\sigma_{sca}}{\sigma_{sca} + \sigma_{abs}} \quad (2)$$

SSA was calculated separately for each of wavelength (450, 525 and 635 nm).

Positive matrix factorization (PMF) Receptor model (Paatero and Tapper, 1994; Paatero, 1997), a commonly employed method was used for apportionment of source strength using speciation data. EPA PMF 5.0 program was applied to scattering and absorption coefficients at three wavelengths, $PM_{2.5}$ and coarse (PM_{10}–$PM_{2.5}$) mode aerosol mass concentration. PMF is a receptor-only, factorization model based on mass conservation which requires no a priori information about factor profiles or time trends. PMF has generally been applied to long-term, low-time-resolution datasets, though there has been a call for greater application of source apportionment techniques to air pollution events to facilitate understanding of specific sources for regulatory purposes (Engel-Co and Weber, 2007).

3. Results and discussion

3.1. General features

Seasonal variations of meteorological parameters are presented in Lihavainen et al. (2016). In general the highest temperatures were in June (37 °C on the average) and the lowest in January (24 °C on the average). Wind direction had very clear diurnal pattern, during nights wind was from east, inland, and during day time, it turned to be from about west (sea breeze), from the Red Sea and the city of Jeddah. From May to September the sea breeze was more pronounced than from October to April. Also the wind speed had a clear diurnal pattern, the nights were typically very calm (typically 1–2 $m\,s^{-1}$) whereas during day time winds were stronger (typically about 4–6 $m\,s^{-1}$).

A statistical overview of aerosol optical properties is presented in Table 1 and data series over the measurement period in Fig. 2. The data coverage of 1 h averages from February 2013 to February 2015 was 89% for σ_{sca} and $\mathring{a}_{sca}$, 87% for σ_{abs} and $\mathring{a}_{abs}$ and 79% for *SSA*. The average σ_{sca} at the wavelength of 525 nm wavelength over the campaign period was 109 Mm^{-1} (S.D. 71 Mm^{-1}), and the average σ_{abs} at the wavelength of was 15 Mm^{-1} (S.D. 17 Mm^{-1}). The average *SSA* was 0.88 (S.D. 0.09). The *SSA* has relatively frequent events with extremely low values below to 0.6 which are related to high σ_{abs} values during nights, Fig. 2.

The average $\mathring{a}_{sca}$ was 0.49 (S.D. 0.62). Relatively low $\mathring{a}_{sca}$ indicates that the size distribution is dominated by coarse mode particles. This was also observed in earlier study where coarse mode particles covered about 70% of PM_{10} mass (Lihavainen et al., 2016). The average $\mathring{a}_{abs}$ was 0.97 (S.D. 0.22). This is typical value for quite fresh BC.

Some general features in seasonal variation of aerosol optical properties were observed. σ_{sca} and σ_{abs} followed the same general behavior, which was characterized by the highest concentrations from February to May, 124 and 18 Mm^{-1} on the average respectively. The lowest values for both σ_{sca} and σ_{abs} were on December and January, 95 and 11 Mm^{-1} on the average, respectively. The seasonal variation of σ_{sca} and σ_{abs} has similar characteristics that were observed for PM_{10} (Lihavainen et al., 2016). The high aerosol mass load and consequent high σ_{sca} and σ_{abs} are related to dust outbreaks and storms which have been reported to occur in the area during this time of the year (e.g. Hussein et al., 2014; Alghamdi et al., 2015).

Single scattering albedo, *SSA*, had the highest values in December and January, 0.89 on the average, and the lowest in May and July, around 0.83. The wavelength dependency of *SSA* was slightly stronger during dust outbreak period as dust absorbs stronger at shorter wavelengths. During dust break period *SSA* varied from 0.87 to 0.89 as a function of wavelength from 450 nm to 635 nm, whereas from July to December, it was almost constant 0.87. The seasonal variation of $\mathring{a}_{sca}$ was noticeable but almost opposite to σ_{sca}, low values from February to May, 0.23, and the highest values from August to December, 0.74. Very low $\mathring{a}_{sca}$ values are indicating that the aerosol size distribution is dominated clearly by large, super micron particles, which were most probably related to dust outbreaks and storms. During the dust outbreak and storm period (from February to May) the aerosol absorption Ångström exponent, $\mathring{a}_{abs}$, was close to one, 1.02 on average. $\mathring{a}_{abs}$ had the lowest values from September to November, 0.90 on average.

The highest values of σ_{sca} (> 500 Mm^{-1}) were typically observed in air with $\mathring{a}_{sca}$ in the range from -0.5 to -1.0 (Fig. 3a). Also this indicates that these episodes were dominated by super micron particles originating most probably from desert dust events. The $\mathring{a}_{sca}$ increases with decreasing particle size. Fig. 3b represents $\mathring{a}_{abs}$, as a function of

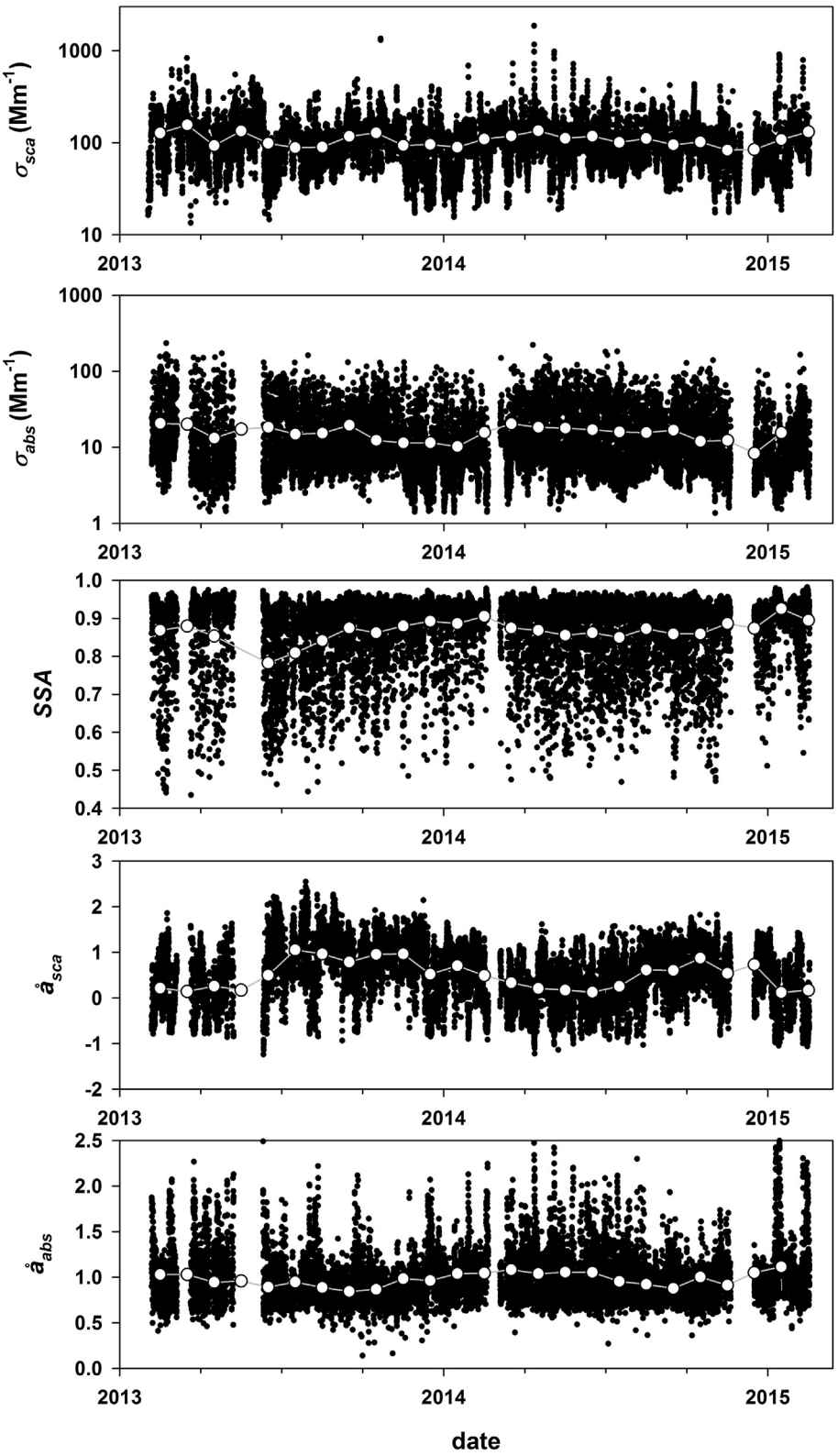

Fig. 2. One hour averages of σ_{sca}, σ_{abs}, single scattering albedo, scattering and absorption Ångström exponents, $å_{sca}$ and $å_{abs}$, over the measurement campaign.

$å_{sca}$. Low $å_{sca}$ values with high $å_{abs}$, > 1.5, were related to dust dominated air masses (Cazorla et al., 2013). The $å_{abs}$ values are decreasing as a function of $å_{sca}$. Values for $å_{abs}$ > 1.5 with $å_{sca}$ > 1.5 were related to OC and sulphate dominated sources. In our measurements $å_{abs}$ was decreasing as a function of $å_{sca}$, at $å_{sca}$ higher than 1.5 the average $å_{abs}$ is 0.88. These values are indicating EC dominated sources.

The average AOD at 500 nm wavelength over measurement period was 0.35 (S.D. 0.2) and $å_{ext}$ 0.72 (S.D. 0.46), Table 1. The $å_{ext}$ is calculated between wavelengths 440 nm and 675 nm. These are standard products from Aeronet, calculating AOD at 525 nm differs only by 2%. The measured AOD values are similar that are measured in the Solar Village in mid Saudi Arabia (e.g. Sabbah and Hasan, 2008) and satellite based measurements at Jeddah region (Yu et al., 2013). The highest hourly averaged values were over 1.0 during the dust season. During

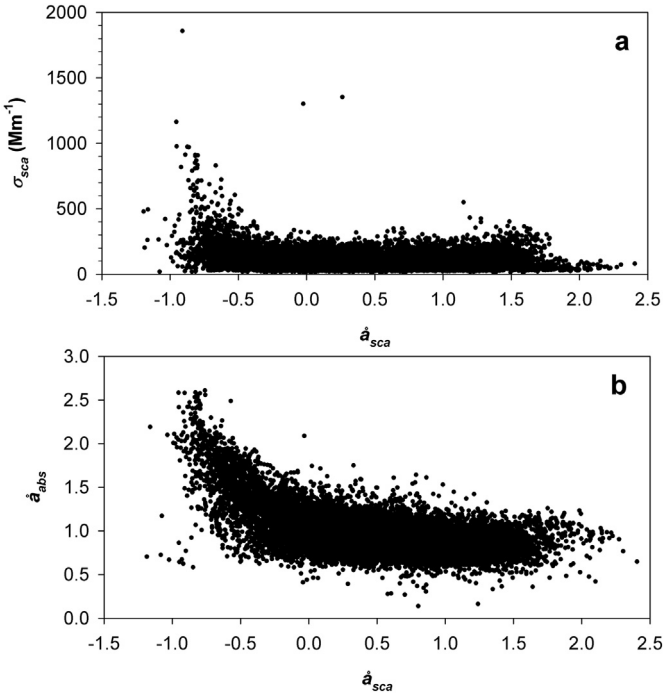

Fig. 3. On the top, a, scattering coefficient σ_{sca}, as a function of scattering Ångström exponent, $å_{sca}$. On the bottom, b, absorption Ångström exponent, $å_{abs}$, as a function of scattering Ångström exponent, $å_{sca}$. Values are one hour averages over the measurement period.

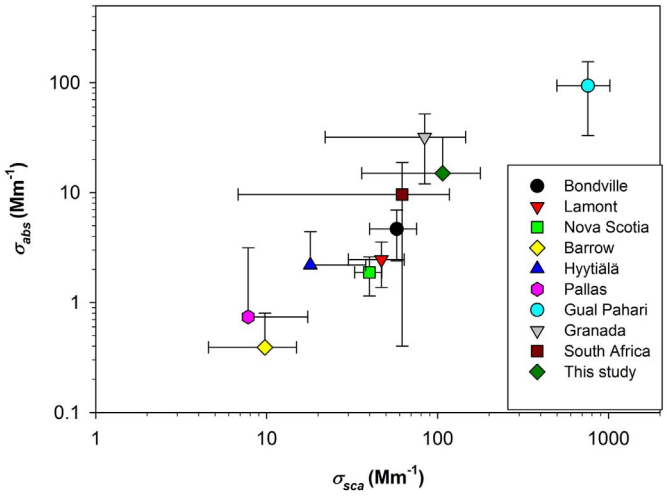

Fig. 4. Comparison of aerosol optical properties in various location over the world, absorption coefficient as a function of scattering coefficient in different location: Bondville, USA (Delene and Ogren, 2002), Lamont, USA (Delene and Ogren, 2002), Nova Scotia, USA (Delene and Ogren, 2002), Barrow, USA (Delene and Ogren, 2002), Hyytiälä, Finland (Virkkula et al., 2011), Pallas, Finland (Lihavainen et al., 2015), Gual Pahari, India (Hyvärinen et al., 2010), Granada, Spain (Lyamani et al., 2008), Elandsfontein, South Africa (Laakso et al., 2012) and this study. Error bars represent standard deviation, negative values are not shown.

these high AOD values $å_{ext}$ were very low, mostly from 0.05 to 0.3, implying again size distribution dominated by large particles. Due to sparse data series, about 25% from optimal, it is not possible to study any seasonal variation.

3.2. Comparison to other sites

To our knowledge there are no prior long term observations of in situ aerosol optical properties from the region. σ_{sca} is quite often reported at 550 nm wavelength. Hence our results were also calculated to 550 nm. This affected only few percent to values in Table 1. The average σ_{sca} and σ_{abs} were compared to published results from some other sites by plotting the averages and standard deviations in a scatter plot (Fig. 4). Delene and Ogren (2002) presented aerosol optical properties from several North American sites. Three of these sites, Barrow, Alaska (representing a background site), the Southern Great Plains Station (SGP), Oklahoma (representing a continental site), and the anthropogenically influenced site Bondville, Illinois (BND) are referenced. Three European stations were also included in the comparison plot. Lyamani et al. (2008) measured σ_{sca} and σ_{abs} at an urban site in Granada, Spain. They measured absorption at 637 nm wavelength, it was extrapolated to 550 nm using the absorption Ångström exponent of 1. Virkkula et al. (2011) presented aerosol optical properties measured at a boreal forest site, SMEAR II, in Finland. Lihavainen et al. (2015) presented aerosol optical properties in Northern Finland on the border of Arctic region. Most polluted region was Gual Pahari in the outskirts of New Delhi (Hyvärinen et al., 2010). They measured σ_{abs} at 637 nm wavelength and σ_{sca} at 525 m, they were extrapolated to 550 nm using the Ångström exponents of 1. Laakso et al. (2012) introduced aerosol optical properties at eastern brink of the heavily polluted Highveld area in South Africa. They reported both σ_{sca} and σ_{abs} at 637 nm. They were extrapolated to 550 nm with scattering Ångström exponent of 1.5 as they reported and assuming absorption Ångström exponent value of 1.

Hada Al Sham has high σ_{sca} and σ_{abs} compared to other sites, Fig. 4. Only in highly polluted area in Indo Gangetic Plain both σ_{sca} and σ_{abs} are clearly higher than in other compared sites. σ_{sca} are quite similar than in urban site in Granada, although the sources are different. In Granada large σ_{sca} values are caused by transport of pollution form Europe and the aerosol in the region contain large fraction of absorbing material. Also the size distribution was clearly different, dominated by fine particles with $å_{sca}$ value of 1.8. In Hada Al Sham σ_{sca} is dominated by the coarse mode desert dust and anthropogenic sulphate particles in $PM_{2.5}$. σ_{abs} is clearly lower than in Granada, closer to that of South Africa. In South Africa the sources of absorbing aerosols are industrial activities, domestic heating and large emissions from the wildfires. At our site σ_{abs} was dominated by high night time values which were more than three times the day time values (see below).

3.3. Diurnal variation

Diurnal variation of σ_{sca} and σ_{abs} was clearly different, Fig. 5. σ_{sca} had two clearly distinguishable peaks (Fig. 5a), quite sharp peak in the morning around 08:00 h and broader peak with lower values in the afternoon from about 17:00 to 20:00 h. During morning peak also $å_{sca}$ was decreasing from above 0.6 to below 0.4 and in the afternoon from day time value of about 0.7 to below 0.5. These features indicate that the morning peak in σ_{sca} and simultaneous sharp decrease in $å_{sca}$ might be related to air movements that lift coarse mode particles from surface which have been deposited during the calm nights. Similar peaks were also observed for PM_{10} and the coarse mode (particles between 2.5 and 10 μm in diameter) mass concentration (Lihavainen et al., 2016). Low level jets (e.g. Allen and Washington, 2014) can also cause the morning peak of σ_{sca} and mass concentrations. Although the surface winds in our site are extremely calm during night time, without measurement of vertical profiles of winds the effect of low level jets cannot be ruled out.

The highest values of σ_{abs} were observed during the night time, from around 02:00 to 09:00 h (Fig. 5b). After 09:00, σ_{abs} decreased steeply from around 22 to around 6 Mm^{-1}. During night time $å_{abs}$ was between 0.8 and 0.85. During day time $å_{abs}$ increased being at the maximum, about 1.1, at around 19:00 h and then again decreases to the night time value. *SSA* followed oppositely σ_{abs}. During night time the *SSA* was lowest, around 0.82, and increased during day time being 0.93 at the highest. Practically all the hourly average values below 0.70 were observed during the night time, lowest one hour averages being about 0.44. This kind of behavior could be due to BC spheres, maybe coated,

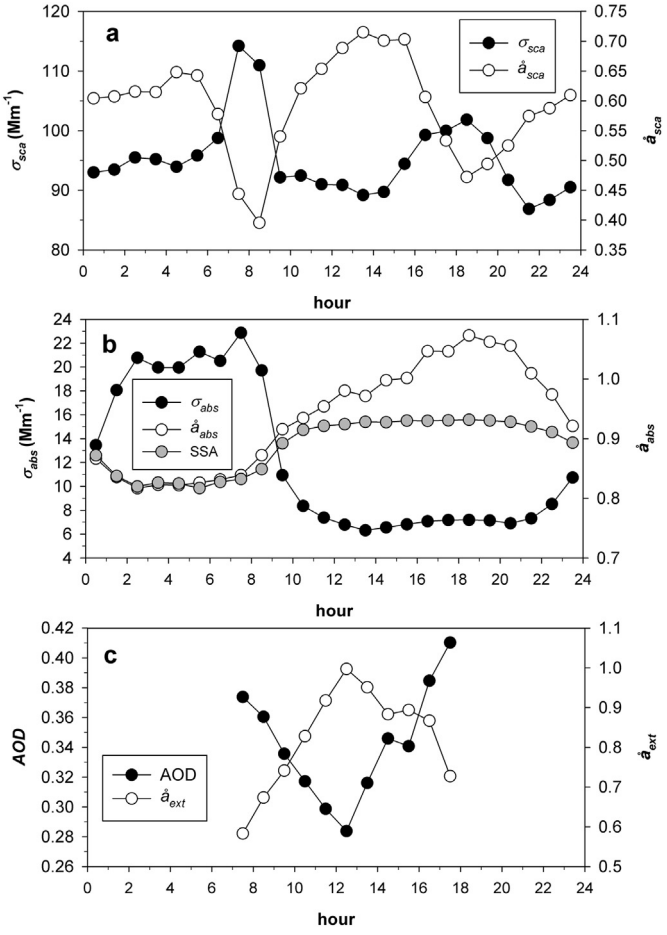

Fig. 5. On the top (a) is diurnal variation of σ_{sca} and $å_{sca}$, at the middle (b) diurnal variation ofσ_{sca}, $å_{abs}$ and SSA and at the bottom (c) diurnal variation of AOD and $å_{ext}$. Values calculated over the campaign period.

that are larger than ~150 nm (Lack and Cappa, 2010; Cazorla et al., 2013).

The daily variation (AOD measurements from about 07:00 to 18:00) of AOD and $å_{ext}$ had similar features than σ_{sca} and $å_{sca}$, high AOD values in the morning decreasing towards the noon and the increasing again towards evening, Fig. 5. The evening AOD values were slightly higher than the morning values. This differs from the σ_{sca}, this might be due to only daylight measurement of AOD and possible aerosol layers occurring at higher altitudes. $å_{ext}$ had low values in the morning and evening again suggesting domination of larger particles in the size distribution. The decrease of AOD during daytime suggests that the evolving boundary layer and consequent enhanced mixing and dilution leading to lower σ_{sca} and σ_{abs}, and mass concentration values measured at ground level, had not strong effect.

3.4. Variation of aerosol optical properties with other measured parameters

Both aerosol σ_{sca} and σ_{abs} varied with respect to wind direction, Fig. 6a and b. σ_{sca} had minimum values when wind was from north, between 300° and 30°. The highest values were from 50° to 270° with one distinguishable peak from wind direction 200°–240°. This direction is towards the southern part of Jeddah where major harbors and heavy industry are located. The distance to this industrial area from our measurement site is about 60 km. Also $å_{sca}$ (Fig. 5a) was higher when wind was from this direction indicating existence of larger fraction of submicron particles than from other wind directions. In earlier study from the site by Lihavainen et al. (2016), it was observed that this wind direction had maximum in total number concentration (concentration

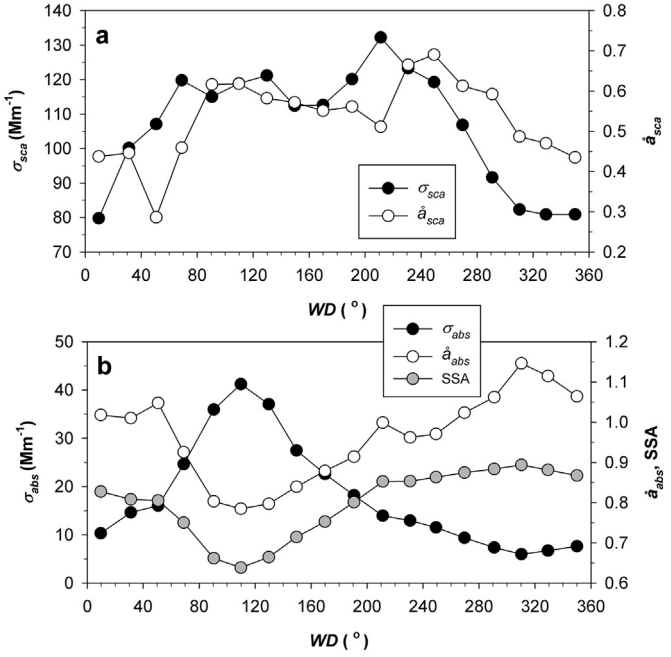

Fig. 6. On top (a) is variation of σ_{sca} and $å_{sca}$ as a function of wind direction (*WD*), and at the bottom (b) variation ofσ_{sca}, $å_{abs}$ and SSA as a function of wind direction. Values are calculated over the campaign period.

of particle larger than 10 nm in diameter). This peak was not observed in PM_{10} or $PM_{2.5}$ concentrations. In the same study it was observed that new particle formation events dominated the number concentration (Lihavainen et al., 2016). The growth of nucleated particles was very strong and the particles grew to accumulation mode where they can also affect scattering coefficient. Sulphur dioxide is known to form sulphuric acid in photochemical processes (e.g. Seinfeld and Pandis, 2006) which can be related to new particle formation and growth (e.g. Sipilä et al., 2010). The largest sources of sulphur dioxide in Jeddah are desalination plant and power plant in center of Jeddah and a lubricant oil manufacturing plant south of Jeddah. The σ_{abs} does not have any distinguishable peak from this direction hence it might be tempting to assume that the particles are sulphate dominated, see also PMF analysis below.

σ_{abs} had also the minimum values in northern air masses, Fig. 6b. Clear peak was observed from winds from 100° to 120°. This was also the direction where the minimum in both $å_{abs}$ and *SSA* was observed, Fig. 6b. Winds were typically from this direction during night time. Winds were very calm during night time, typically between 1 and 2 m s^{-1}, which would indicate to some local source. The reason for high σ_{abs} during the night time is still unclear. This sector 100°–120° did not contain buildings, major roads or other obvious aerosol sources.

The variation of σ_{sca} with wind speed was quite typical for this kind of surroundings, Fig. 7a. $å_{sca}$ is also decreasing as a function of wind speed, average being below zero at winds 9–10 m s^{-1}. There are not enough of statistics for higher wind speed values, but if the chosen limit of 100 values with wind speed bin is lowered to 20 the increase at higher wind speeds (11–12 m s^{-1}) is more pronounced, σ_{sca} being around 220 Mm^{-1} (S.D. 198 Mm^{-1}) and $å_{sca}$ around −0.55 (S.D. 0.24). The high scattering coefficients and low $å_{sca}$ values during higher wind speeds are most likely due to dust loads transported from the surrounding desert areas. The variation of σ_{abs} is almost opposite than σ_{sca} at wind speeds higher than 2 m s^{-1}, Fig. 7b. $å_{abs}$ is increasing as function of wind speed indicating also domination of large dust particles. The variation of absorption coefficient and $å_{abs}$ was related to calm night time higher concentrations, Fig. 5b and previous paragraph.

The variation of aerosol optical properties with temperature and relative humidity were dominated by diurnal cycle of land and sea

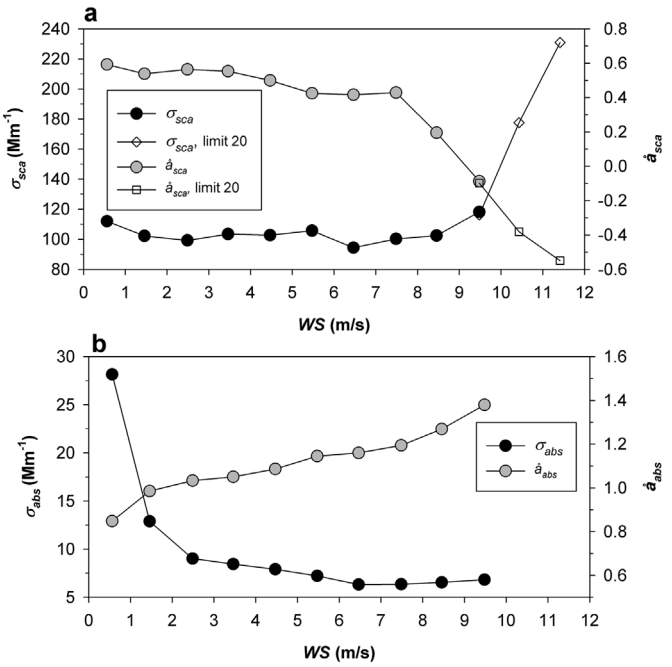

Fig. 7. On top (a) is variation of σ_{sca} and $å_{sca}$ as a function of wind speed (*WS*), and at the bottom (b) variation ofσ_{sca} and $å_{abs}$ as a function of *WS*. Values are calculated over the campaign period.

breeze and desert dust event season in spring time. It does not bring any additional information and it is left out from analysis.

σ_{sca} and σ_{abs} were compared to PM_{10}, $PM_{2.5}$ and coarse (PM_{10}–$PM_{2.5}$) mode concentration and aerosol optical depth (AOD), all measured at the site, Table 2. There was a clear linear relationship with scattering coefficient and PM_{10} concentrations. The correlation coefficient, R, with scattering coefficient and PM_{10} was 0.88. The correlation with scattering coefficient and $PM_{2.5}$ concentration was weaker, R = 0.59. For coarse mode (PM_{10}–$PM_{2.5}$) was R = 0.83. This clearly demonstrates the domination of super micron particles on the scattering coefficient. The correlation coefficient between AOD and σ_{sca} was fairly good, R = 0.68, considering that the AOD is a value measured over the whole atmospheric column, in situ measurement were made at RH < 50% conditions. AOD is a related to sum of scattering and absorption (extinction), the correlation with σ_{sca} + σ_{abs} and AOD is a bit weaker, R = 0.64, than just with scattering. Even though the fraction of absorption from extinction (σ_{sca} + σ_{abs}) was about 20% (at ground level) there was no correlation with σ_{abs} and AOD.

3.5. PMF analysis

σ_{sca} and σ_{abs} at three wavelengths and $PM_{2.5}$ and the coarse (PM_{10}–$PM_{2.5}$) mode mass concentrations (Lihavainen et al., 2016) were used to identify source characteristics and contributions with PMF analysis. Three scientifically sound factors with clearly different characteristics were found, Table 3. For simplicity we assume here that the aerosol is more externally mixed, three factors and their combinations. Diurnal variation of contribution of factors is presented in Fig. 8a and variation of contribution of factors with wind direction in Fig. 8b. In

Table 2
Correlation of aerosol optical properties with other measured parameters.

	AOD (500 nm)	$PM_{2.5}$	PM_{10}	Coarse
σ_{sca} (525 nm)	0.68	0.59	0.88	0.83
σ_{abs} (525 nm)	0.23	0.13	0.21	0.20
σ_{sca} + σ_{abs}	0.64	0.54	0.81	0.76

Table 3
Optical properties of source characteristics with PMF analysis. σ_{sca} and σ_{abs} in Mm^{-1} and $PM_{2.5}$ and coarse mode concentrations in μg m^{-3}.

	Factor 1 Anthropogenic	Factor 2 BC source	Factor 3 Desert dust
σ_{sca} (450 nm)	64	10	30
σ_{sca} (525 nm)	49	7	38
σ_{sca} (635 nm)	34	5	44
σ_{abs} (450 nm)	0.3	16.7	2.5
σ_{abs} (525 nm)	0.2	15.0	1.9
σ_{abs} (635 nm)	0.1	13.1	1.3
$PM_{2.5}$	19.5	2.2	3.5
Coarse	3.6	0.3	47.5
$å_{sca}$	1.9	2.4	− 1.1
$å_{abs}$	3.2	0.7	1.9
SSA	0.99	0.35	0.95

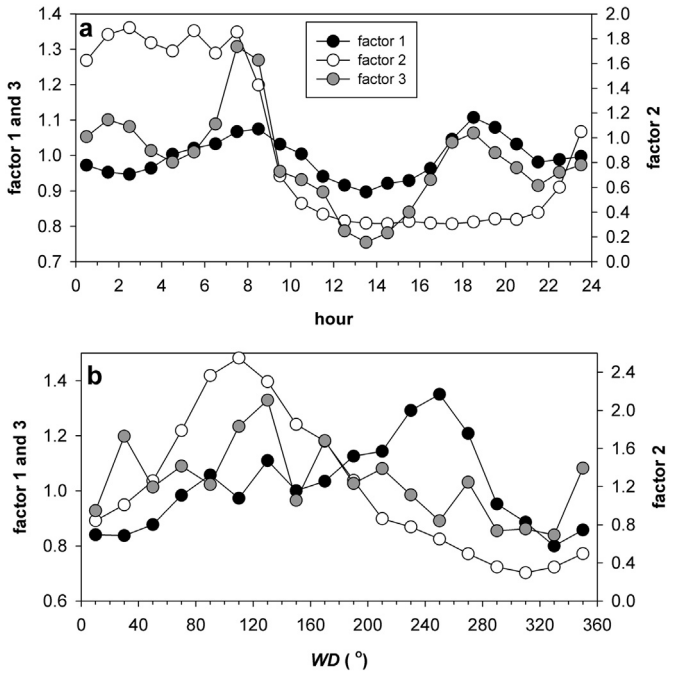

Fig. 8. On top (a) is diurnal variation of factors 1–3 and at the bottom (b) variation of factors 1–3 as a function of wind direction (WD). Values are calculated over the campaign period.

Fig. 8a and b the average of contribution over the variable is one.

Factor 1 is dominated by concentration of particles smaller than 2.5 μm, this is named as anthropogenic factor. The seasonal variation of contribution of factor 1 is quite evenly distributed with small minimum on June and July. The *SSA* of this factor is very close to unity since σ_{abs} is very low. In diurnal variation there are two distinguishable peaks, Fig. 8a, small one in the morning around 08:00 to 10:00 h and a bigger and longer lasting one in the afternoon forming around 16:00 to 20:00 h. From variation of contribution of factor 1 with wind direction one can observe that factor 1 has the highest contribution from wind sector 200°–260°, Fig. 8b. This direction is towards southern part of Jeddah where major harbors and heavy industry are located. The $å_{sca}$ is 1.9 indicating fine particle dominated size distribution. $å_{abs}$ is 3.2, indicating that absorption is dominated by OC sources (Cazorla et al., 2013) but because the σ_{abs} is very low OC has practically no contribution to this factor. Sulphate is essentially an entirely scattering aerosol across the solar spectrum (Penner et al., 2001) this factor represents mostly sulphate aerosols having major source areas from Jeddah. The mass scattering efficiency of this factor is 2.5 m^2 g^{-1} for $PM_{2.5}$. This agrees to values reported in a review for ammonium sulphate aerosols, mean 2.5 ± 0.6 m^2 g^{-1} for PM_1 or $PM_{2.5}$ (Hand and

Malm, 2007).

Factor 2 is dominated by absorption, a BC source factor. The mass concentration is also dominated by $PM_{2.5}$ particles but the concentrations are clearly lower than in factor 1, i.e. $PM_{2.5}$ values 10 times lower. Scattering coefficients area also about 10 times lower than in factor 1. Seasonal variation is similar than σ_{abs}. Diurnal variation, Fig. 8a, clearly shows that the major contribution of the factor is during night time. Also the variation of contribution with respect to variation with wind direction is very similar to the absorption coefficient in Fig. 8b. The $å_{sca}$ is highest of all factors, 2.4, whereas the $å_{abs}$ is the lowest, 0.7. High $å_{sca}$ indicates that the aerosol size distribution is dominated by submicron particles, smaller than in factors 1 and 3. The emission sources of BC are combustion processes of fossil and non-fossil carbonaceous fuels. $å_{abs}$ values below one are commonly related to traffic emissions (e.g. Zotter et al., 2017; Herich et al., 2011). Hence also BC source factor is of anthropogenic origin, most probably diesel vehicles or generator. The mass absorption efficiency is 6.0 $m^2 g^{-1}$. This is quite close to value reported value representative of BC in Central Europe 5.3 $m^2 g^{-1}$ (Nordmann et al., 2013) and for uncoated BC aerosol 7.5 ± 1.2 $m^2 g^{-1}$ (Bond and Bergstrom, 2006).

Factor 3 is a desert dust factor, the particle mass is totally in coarse mode. The $å_{sca}$ is the lowest, − 1.1, and $å_{abs}$ is highest, 1.9, compared to factors 1 and 2. This also points towards desert dust dominated factor (Cazorla et al., 2013). The seasonal variation of contribution of factor 3 has clearly higher values from February to May when the desert dust episode season at the area occurs. Diurnal variation of contribution of factor 3 has clear morning peak between 08:00 and 10:00 h, then contribution decreases to its minimum value at 15:00 h. This indicates that the morning peak of σ_{sca}, Fig. 5, is caused by desert dust whereas the afternoon peak is also caused by anthropogenic activities (see above and Lihavainen et al., 2016). The variation of contribution of desert dust factor with wind direction is quite uniform indicating that the desert dust sources are all-around, as it is. There is a slight peak from wind direction from 110° to 140° which is related to morning peak. The mass absorption efficiency of this factor is 0.04 $m^2 g^{-1}$. This is close to the value measured for dust during EAST-AIRE (East Asian Study of Tropospheric Aerosols: an International Regional Experiment) campaign near Beijing 0.03 $m^2 g^{-1}$ (Yang et al., 2009) and soil samples analyzed from Gobi, Sahara and Sahel deserts 0.01–0.02 $m^2 g^{-1}$ (Alfaro et al., 2004). Mass scattering efficiency of this factor is 0.8 $m^2 g^{-1}$ which agrees to values reported for Neveg Desert in Israel, 0.52 ± 0.03 $m^2 g^{-1}$ (Andreae et al., 2002), and from a cruise from Norfolk to Cape Town, 0.9 $m^2 g^{-1}$ (Quinn et al., 2001).

4. Conclusions

Aerosol scattering, σ_{sca}, and absorption, σ_{abs}, coefficients were measured at a rural background area in the Western Saudi Arabia. Data analyzed here covers time frame from February 2013 to February 2015. Both σ_{sca}, and σ_{abs} showed clear seasonal variation. The variation was related to dust storms occurring in the area from February to March. Scattering Ångström exponent, $å_{sca}$, had also clearly lower value and absorption Ångström exponent, $å_{abs}$, clearly higher values in this time period indicating size distribution dominated clearly by dust like super micron particles.

Diurnal variation of σ_{sca}, and σ_{abs} were clearly different. σ_{sca} had two clear peaks, in the morning and late afternoon. PMF analysis revealed that the morning peak is dominated by desert dust whereas the afternoon peak was evenly influenced by anthropogenic emissions from the city of Jeddah. σ_{abs} was three times higher during night time than during day time. $å_{abs}$ was also very low during night time, about 0.8, compared to day time. $å_{abs}$ values below one have been related to traffic (e.g. Zotter et al., 2017; Herich et al., 2011) This indicates that these high night time σ_{abs} values are of anthropogenic origin but any obvious source could not be identified. The decrease of AOD during daytime suggest that the evolving boundary layer and consequent enhanced mixing and dilution leading to lower σ_{sca} and σ_{abs}, and mass concentration values measured at ground level did not have strong effect.

Diurnal variation was also reflected to variation of aerosol optical properties with wind direction and speed due to the consistent diurnal pattern of the winds throughout the year: very calm nights with westerly wind and sea breeze from Red Sea, east, during day time. σ_{sca} was quite steadily high from 50° to 270°, having a peak from 200° to 240°. Diurnal variation is very similar than variation of PM_{10} concentrations (Lihavainen et al., 2016). PMF analysis revealed that the peak is probably from anthropogenic activities whereas the steady high values from about 50° to 200° was dust dominated. σ_{abs} had a clear maximum from 100° to 120°, this is the night time peak.

To our knowledge we used PMF analysis for the first time to optical and physical properties to study characteristics of aerosols from different sources. Analysis revealed three clearly different types of sources, anthropogenic, BC source and desert dust. These factors have clearly different seasonal and diurnal variation. The contribution of desert dust factor was dominating from February to May, whereas the contribution of anthropogenic factor is quite steady over the whole year. The night time factor follows the same pattern than σ_{abs}. We estimated the mass absorption and scattering efficiencies for the factors and they agreed well with earlier observations. Hence, this method could be used to distinguish aerosol source characteristics, at least in fairly simple cases.

σ_{sca} correlated with PM_{10} and coarse mode concentrations because of desert dust as expected. σ_{abs} did not correlate with particle mass concentrations at all, it is dominated with clearly smaller particles than σ_{sca}. From PMF analysis BC source factor was identified which is absorption dominated, the size parameter $å_{sca}$ was highest of three factor, 2.4. This also support the fact that σ_{abs} is dominated by small, submicron particles. σ_{sca} correlated quite nicely also with AOD measured at the site. σ_{abs} did not correlate with AOD, which was expected since during day time extinction is dominated by scattering.

The aerosol optical properties in Western Saudi Arabia are dominated by desert dust, but anthropogenic activities play an important role as well. At our measurement site the aerosol climatology is driven seasonally by dust season most active from February to May and diurnally by uniform pattern in wind speed and especially direction.

Acknowledgements

This study was funded by the Deanship of Scientific Research (DSR), King Abdulaziz University (KAU), Jeddah, under grant no. I-122-430. The authors acknowledge with thanks DSR and KAU for technical and financial support. We also like to acknowledge Centre of Excellence program (project no 1118615) of Academy of Finland.

References

Alam, K., Trautmann, T., Blaschke, T., Subhan, F., 2014. Changes in aerosol optical properties due to dust storms in the Middle East and Southwest Asia. Remote Sens. Environ. 143, 216–227.

Alfaro, S.C., Lafon, S., Rajot, J.L., Formenti, P., Gaudichet, A., Maillé, M., 2004. Iron oxides and light absorption by pure desert dust: an experimental study. J. Geophys. Res. 109, D08208. http://dx.doi.org/10.1029/2003JD004374.

Alghamdi, M.A., Almazroui, M., Shamy, M., Redal, M.A., Alkhalaf, A.K., Hussein, M.A., Khoder, M.I., 2015. Characterization and elemental composition of atmospheric aerosol loads during springtime dust storm in Western Saudi Arabia. Aerosol Air Qual. Res. 15, 440–453.

Allen, C.J.T., Washington, R., 2014. The low-level jet dust emission mechanism in the central Sahara: observations from Bordj-Badji Mokhtarduring the June 2011 Fennec Intensive Observation Period. J. Geophys. Res. Atmos. 119, 2990–3015. http://dx.doi.org/10.1002/2013JD020594.

Andreae, T.W., Andreae, M.O., Ichoku, C., Maenhaut, W., Cafmeyer, J., Karnieli, A., Orlovsky, L., 2002. Light scattering by dust and anthropogenic aerosol at a remote site in the Negev desert, Israel. J. Geophys. Res. 107 (D2), 4008. http://dx.doi.org/10.1029/2001JD900252.

Bergstrom, R.W., Pilewskie, P., Russell, P.B., Redemann, J., Bond, T.C., Quinn, P.K., Sierau, B., 2007. Spectral absorption properties of atmospheric aerosols. Atmos. Chem. Phys. 7, 5937–5943.

Bond, T.C., Bergstrom, R.W., 2006. Light absorption by carbonaceous particles: an investigative review. Aerosol Sci. Technol. 40 (1), 27–67. http://dx.doi.org/10.1080/

02786820500421521.
Cazorla, A., Bahadur, R., Suski, K.J., Cahill, J.F., Chand, D., Schmid, B., Ramanathan, V., Prather, K.A., 2013. Relating aerosol absorption due to soot, organic carbon, and dust to emission sources determined from in-situ chemical measurements. Atmos. Chem. Phys. 13, 9337–9350. http://dx.doi.org/10.5194/acp-13-9337-2013. www.atmos-chem-phys.net/13/9337/2013/.
Charlson, R.J., Schwartz, S.E., Hales, J.M., Cess, R.D., Coakley Jr., J.A., Hansen, J.E., Hoffman, D.J., 1992. Climate forcing by anthropogenic aerosols. Science 255, 423–430.
Collaud Coen, M., Andrews, E., Asmi, A., Baltensperger, U., Bukowieck, N., Day, D., Fiebig, M., Fjaeraa, A.M., Flentje, H., Hyvärinen, A., Jefferson, A., Jennings, S.G., Kouvarakis, G., Lihavainen, H., Lund Myhre, C., Malm, W.C., Mihapopoulos, N., Molenar, J.V., O'Dowd, C., Ogren, J.A., Schichtel, B.A., Sheridan, P., Virkkula, A., Weingartner, E., Weller, R., Laj, P., 2013. Aerosol decadal trends – part 1: in-situ optical measurements at GAW and IMPROVE stations. Atmos. Chem. Phys. 13, 869–894.
Delene, D.J., Ogren, J.A., 2002. Variability of aerosol optical properties at four North American surface monitoring sites. J. Atmos. Sci. 59, 1135–1150.
Engel-Co, J., Weber, S.A., 2007. Compilation and assessment of recent positive matrix factorization and UNMIX receptor model studies on fine particulate matter source apportionment or the eastern United States. J. Air Waste Manage. Assoc. 57, 1307–1316. http://dx.doi.org/10.3155/1047-3289.57.11.1307.
Hand, J.L., Malm, W.C., 2007. Review of aerosol mass scattering efficiencies from ground-based measurements since 1990. J. Geophys. Res. 112, 1–24.
Haywood, J.M., Shine, K.P., 1995. The effect of anthropogenic sulfate and soot aerosol on the clear sky planetary radiation budget. Geophys. Res. Lett. 22, 603–606.
Herich, H., Hueglin, C., Buchmann, B., 2011. A 2.5 year's source apportionment study of black carbon from wood burning and fossil fuel combustion at urban and rural sites in Switzerland. Atmos. Meas. Tech. 4, 1409–1420. http://dx.doi.org/10.5194/amt-4-1409-2011.
Holben, B.N., Eck, T.F., Slutsker, I., Tanré, D., Buis, J.P., Setzer, A., Vermote, E., Reagan, J.A., Kaufman, Y.J., Nakajima, T., Lavenu, F., Jankowiak, I., Smirnov, A., 1998. AERONET — a federated instrument network and data archive for aerosol characterization. Remote Sens. Environ. 66, 1–16.
Hussein, T., Khoder, M., Abdel Maksoud, A.S., Al-Jeelani, H., Alghamdi, M.A., Shabbaj, I.I., Goknil, M.K., Hyvärinen, A., Lihavainen, H., Hämeri, K., 2014. Particulate matter and number concentrations of particles larger than 0.25 μm in the urban atmosphere of Jeddah, Saudi Arabia. Aerosol Air Qual. Res. 14, 1383–1391.
Hyvärinen, A.-P., Lihavainen, H., Komppula, M., Panwar, T.S., Sharma, V.P., Hooda, R.K., Viisanen, Y., 2010. Aerosol measurements at the Gual Pahari EUCAARI station: preliminary results from first year in-situ measurements. Atmos. Chem. Phys. 10, 7241–7252.
IPCC, 2013. Climate change 2013: the physical science basis. In: Contribution of Working Group I to the Fifth Assessment Report of the Intergovernmental Panel on Climate Change. Cambridge University Press, Cambridge, United Kingdom and New York.
Johansen, A.M., Siefert, R.L., Hoffmann, M.R., 1999. Chemical characterization of ambient aerosol collected during the southwest monsoon and intermonsoon seasons over the Arabian Sea: anions and cations. J. Geophys. Res. 104, 26325–26347.
Kaufman, Y.J., Boucher, O., Tanré, D., Chin, M., Remer, L.A., Takemura, T., 2005. Aerosol anthropogenic component estimated from satellite data. Geophys. Res. Lett. 32, L17804. http://dx.doi.org/10.1029/2005GL023125.
Khodeir, M., Shamy, M., Alghamdi, M., Zhong, M., Sun, H., Costa, M., Chen, L.-C., Maciejczyk, P., 2012. Source apportionment and elemental composition of PM2.5 and PM10 in Jeddah City, Saudi Arabia. Atm. Pollut. Res. 3, 331–340. http://dx.doi.org/10.5094/APR.2012.037.
Kim, D., Chin, M., Yu, H., Eck, T.F., Sinyuk, A., Smirnov, A., Holben, B.N., 2011. Dust optical properties over North Africa and Arabian Peninsula derived from the AERONET dataset. Atmos. Chem. Phys. 11, 10733–10741. http://dx.doi.org/10.5194/acp-11-10733-2011.
Kirchstetter, T.W., Novakov, T., Hobbs, P.V., 2004. Evidence that the spectral dependence of light absorption by aerosols is affected by organic carbon. J. Geophys. Res. 109, D21208. http://dx.doi.org/10.1029/2004JD004999.
Laakso, L., Vakkari, V., Laakso, H., Virkkula, A., Kulmala, M., Beukes, J.P., van Zyl, P.G., Pienaar, J.J., Chiloane, K., Gilardoni, S., Vignati, E., Wiedensohler, A., Tuch, T., Birmili, W., Piketh, S., Collett, K., Fourie, G.D., Komppula, M., Lihavainen, H., de Leeuw, G., Kerminen, V.-M., 2012. South African EUCAARI measurements: seasonal variation of trace gases and aerosol optical properties Atmos. Chem. Phys. 12, 1847–1864. http://dx.doi.org/10.5194/acp-12-1847-2012.
Lack, D.A., Cappa, C.D., 2010. Impact of brown and clear carbon on light absorption enhancement, single scatter albedo and absorption wavelength dependence of black carbon. Atmos. Chem. Phys. 10, 4207–4220. http://dx.doi.org/10.5194/acp-10-4207-2010.
Lack, D.A., Cappa, C.D., Covert, D.S., Baynard, T., Massoli, P., Sierau, B., Bates, T.S., Quinn, K., Lovejoy, E.R., Ravishankara, A.R., 2008. Bias in filter based aerosol light absorption measurements due to organic aerosol loading: evidence from ambient measurements. Aerosol Sci. Technol. 42, 1033–1041.
Lelieveld, J., et al., 2001. The Indian Ocean Experiment: Widespread air pollution from South and Southeast Asia. Science 291, 1031–1036.
Lihavainen, H., Hyvärinen, A., Asmi, E., Hatakka, J., Viisanen, Y., 2015. Long-term variability of aerosol optical properties in northern Finland. Boreal Environ. Res. 20, 526–541.
Lihavainen, H., Alghamdi, M.A., Hyvärinen, A.-P., Hussein, T., Aaltonen, V., Abdelmaksoud, A.S., Al-Jeelani, H., Almazroui, M., Almehmadi, F.M., Al Zawad, F.M., Hakala, J., Khoder, M., Neitola, K., Petäjä, T., Shabbaj, I.I., Hämeri, K., 2016. Aerosols physical properties at Hada Al Sham, western Saudi Arabia. Atmos. Environ. 135, 109–117.
Lyamani, H., Olmo, F.J., Alodo-Arboleda, L., 2008. Light scattering and absorption properties of aerosol particles in the urban environment of Granada, Spain. Atmos. Environ. 42, 2630–2642.
Müller, T., Laborde, M., Kassell, G., Wiedensohler, A., 2011. Design and performance of a three-wavelength LED-based total scatter and backscatter integrating nephelometer. Atmos. Meas. Tech. 4, 1291–1303.
Nordmann, S., Birmili, W., Weinhold, K., Müller, K., Spindler, G., Wiedensohler, A., 2013. Measurements of the mass absorption cross section of atmospheric soot particles using Raman spectroscopy. J. Geophys. Res. Atmos. 118, 12,075–12,085. http://dx.doi.org/10.1002/2013JD020021.
Osipov, S., Stenchikov, G., Brindley, H., Banks, J., 2015. Diurnal cycle of the dust instantaneous direct radiative forcing over the Arabian Peninsula. Atmos. Chem. Phys. 15, 9537–9553. http://dx.doi.org/10.5194/acp-15-9537-2015.
Paatero, P., 1997. Least squares formulation of robust non-negative factor analysis. Chemom. Intell. Lab. 37, 23–35.
Paatero, P., Tapper, U., 1994. Positive Matrix Factorization: a non-negative factor model with optimal utilization of error estimates of data values. Environmetrics 5, 111–126.
Penner, J.E., et al., 2001. Aerosols, their direct and indirect effects. In: Houghton, J.T. (Ed.), Climate Change 2001: The Scientific Basis. Contribution of Working Group I to the Third Assessment Report of the Intergovernmental Panel on Climate Change. Cambridge University Press, Cambridge, United Kingdom and New York, NY, USA, pp. 289–348.
Prospero, J.M., Ginoux, P., Torres, O., Nicholson, S.E., Gill, T.E., 2002. Environmental characterization of global sources of atmospheric soil dust identified with the nimbus 7 total ozone mapping spectrometer (TOMS) absorbing aerosol product. Rev. Geophys. 40 (1), 1002. http://dx.doi.org/10.1029/2000RG000095.
Quinn, P.K., Coffman, D.J., Bates, T.S., Miller, T.L., Johnson, J.E., Voss, K., Welton, E.J., Neususs, C., 2001. Dominant aerosol chemical components and their contribution to extinction during the Aerosols99 cruise across the Atlantic. J. Geophys. Res. 106 (D18), 20,783–20,809.
Ramanathan, V., Ramana, M.V., Roberts, G., Kim, D., Corrigan, C., Chung, C., Winker, D., 2007. Warming trends in Asia amplified by brown cloud solar absorption. Nature 448. http://dx.doi.org/10.1038/nature06019.
Sabbah, I., Hasan, F.M., 2008. Remote sensing of aerosols over the Solar Village, Saudi Arabia. Atmos. Res. 90, 170–179.
Sabbah, I., Humood, F.F., Al-Kandari, A., Al-Sharifi, F., 2012. Remote sensing of desert dust over Kuwait: long–term variation. Atmos. Pollut. Res. 3, 95–104.
Schwarze, P.E., Øvrevik, J., Låg, M., Refsnes, M., Nafstad, P., Hetland, R.B., Dybing, E., 2006. Particulate matter properties and health effects: consistency of epidemiological and toxicological studies. Hum. Exp. Toxicol. 25, 559–579.
Seinfeld, J.H., Pandis, S.N., 1998. Atmospheric Chemistry and Physics: From Air Pollution to Climate Change. John Wiley & Sons, New York.
Seinfeld, J., Pandis, S., 2006. Atmospheric Chemistry and Physics, II edition. John Wiley Sons, Inc.
Sipilä, M., Berndt, T., Petäjä, T., Brus, D., Vanhanen, J., Stratmann, F., Patokoski, J., Mauldin III, R.L., Hyvärinen, A., Lihavainen, H., Kulmala, M., 2010. The role of sulfuric acid in atmospheric nucleation. Science 327, 1243. http://dx.doi.org/10.1126/science.1180315.
Virkkula, A., Backman, J., Aalto, P.P., Hulkkonen, M., Riuttanen, L., Nieminen, T., Dal Maso, M., Sogacheva, L., de Leeuw, G., Kulmala, M., 2011. Seasonal cycle, size dependencies, and source analyses of aerosol optical properties at the SMEAR II measurement station in Hyytiälä, Finland. Atmos. Chem. Phys. 11, 4445–4468.
Weingartner, E., Saathoff, H., Schnaiter, M., Streit, N., Bitnar, B., Baltensperger, U., 2003. Absorption of light by soot particles: determination of the absorption coefficient by means of aethalometers. J. Aerosol Sci. 34 (1445–1463), 2003.
WMO/GAW Aerosol measurement procedures: guidelines and recommendations. GAW report number 227. 2016.
Yang, M., Howell, S.G., Zhuang, J., Huebert, B.J., 2009. Attribution of aerosol light absorption to black carbon, brown carbon, and dust in China – interpretations of atmospheric measurements during EAST-AIRE. Atmos. Chem. Phys. 9, 2035–2050. http://dx.doi.org/10.5194/acp-9-2035-2009.
Yu, Y., Notaro, M., Liu, Z., Kalashnikova, O., Alkolibi, F., Fadda, E., Bakhrjy, F., 2013. Assessing temporal and spatial variations in atmospheric dust over Saudi Arabia through satellite, radiometric, and station data. J. Geophys. Res. Atmos. 118, 13,253–13,264. http://dx.doi.org/10.1002/2013JD020677.
Zotter, P., Herich, H., Gysel, M., El-Haddad, I., Zhang, Y., Močnik, G., Hüglin, C., Baltensperger, U., Szidat, S., Prévôt, A.S.H., 2017. Evaluation of the absorption Ångström exponents for traffic and wood burning in the aethalometer-based source apportionment using radiocarbon measurements of ambient aerosol. Atmos. Chem. Phys. 17, 4229–4249. http://dx.doi.org/10.5194/acp-17-4229-2017.